

Supporting Information

Efficiency optimization of BaY₂Al_{2-y}Sc_yGa₂SiO₁₂:xCr³⁺ garnet phosphors with sustained anti-thermal quenching behavior

Haiyan Shi, Yan Yuan, Desheng Yin, Xiaohong Zhang, Pengbo Lyu*, Changfu Xu*, Lizhong Sun*

Hunan Provincial Key Laboratory of Thin Film Materials and Devices, School of Material Sciences and Engineering, Xiangtan University, Xiangtan 411105, People's Republic of China

E-mail: pengbo.lyu@xtu.edu.cn (P. Lyu), xcf@xtu.edu.cn (C. Xu), lzsun@xtu.edu.cn (L. Sun)

Computational methods

First-Principles Calculations

We conducted all first-principles calculations using the Vienna Ab Initio Simulation Package (VASP) at density functional theory (DFT) level¹. Exchange-correlation energy was treated using Perdew-Burke-Ernzerhof (PBE) functional within the generalized gradient approximation (GGA) scheme^{2,3}. The super cell for BaY₂Al₂Ga₂SiO₁₂:Cr³⁺ and BaY₂Al_{1.5}Sc_{0.5}Ga₂SiO₁₂:Cr³⁺, comprising 160 atoms each, were consistently employed for structure relaxations and the calculation of Debye temperature. The wave function was expanded using a plane-wave basis set with a kinetic energy cut-off of 500 eV, and a k-point mesh of 2×2×2 was chosen for Brillouin zone sampling during structure relaxations. During this process, both the lattice constants and atomic positions were fully relaxed. The force convergence threshold was set at 0.01 eV/Å, while the electron self-consistent convergence threshold is 1×10⁻⁶ eV. The Debye temperature was calculated based on established theories⁴⁻⁶ and obtained via post-processing using VASPKIT⁷.

Transition dipole moment

The transition electric dipole moment (TDM) can be obtained by the following relation⁷:

$$P_{a \rightarrow b} = \langle \psi_b | \mathbf{r} | \psi_a \rangle = \frac{i\hbar}{(E_b - E_a)m} \langle \psi_b | \mathbf{p} | \psi_a \rangle \quad (1)$$

the TDM or dipole transition matrix elements $P_{a \rightarrow b}$, is the electric dipole moment associated with a transition between the initial state a and the final state b . The ψ_a and ψ_b are energy eigenstates with energy E_a and E_b ; m is the mass of the electron. The transition probability between two states is determined by the sum of squares of calculated TDM (P^2).

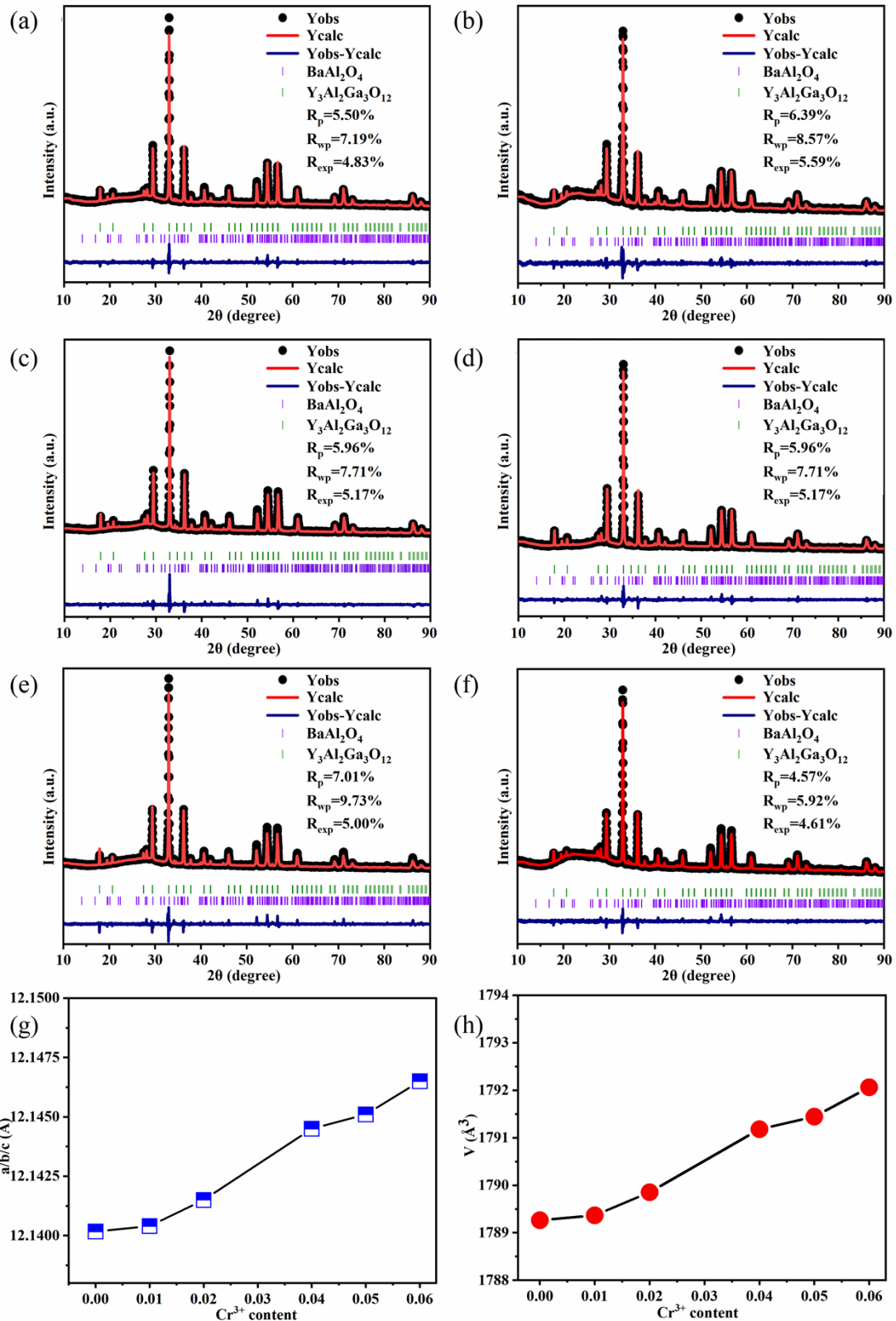


Figure S1. Rietveld refinement XRD patterns of AG: x Cr³⁺ (a) $x = 0$; (b) $x = 0.01$; (c) $x = 0.02$; (d) $x = 0.04$; (e) $x = 0.05$; (f) $x = 0.06$; (g)(h) Changes in lattice parameters (a , b , c , and V) with the Cr³⁺ content.

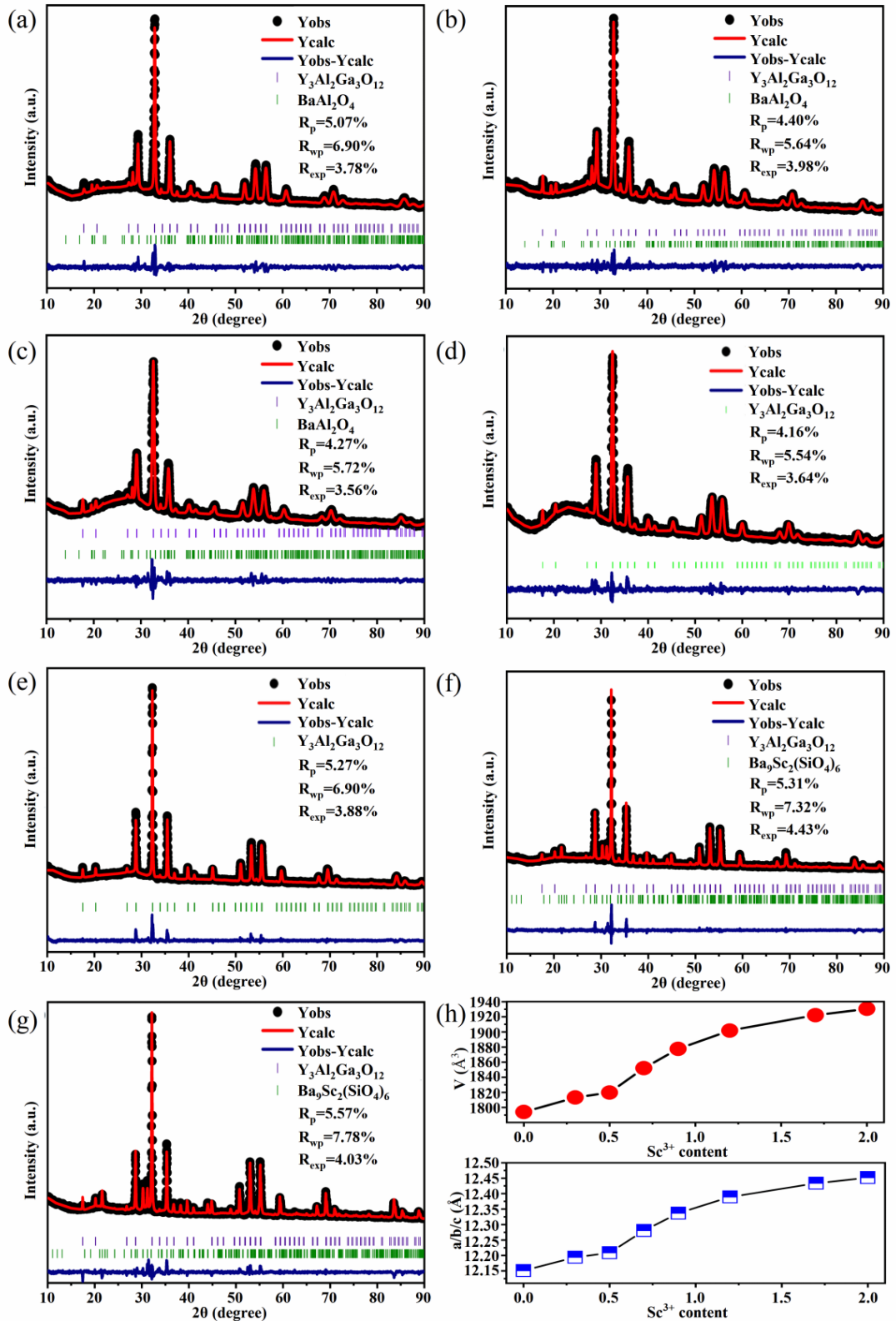


Figure S2. Rietveld refinement XRD patterns of $\text{A}_{2-y}\text{S}_y\text{G}:0.05 \text{Cr}^{3+}$ (a) $y = 0.3$; (b) $y = 0.5$; (c) $y = 0.7$; (d) $y = 0.9$; (e) $y = 1.2$; (f) $y = 1.7$; (g) $y = 2$; (h) Changes in lattice parameters (a, b, c, and V) with the Sc^{3+} content.

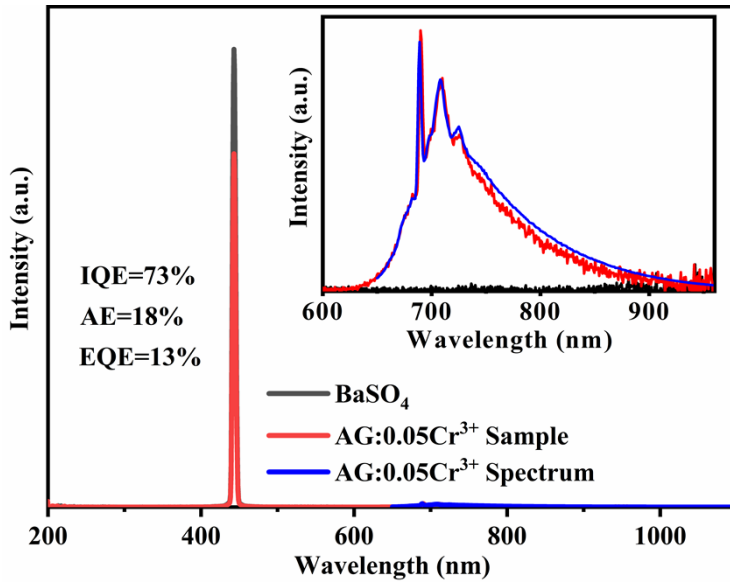


Figure S3. The quantum yield of AG:0.05Cr³⁺

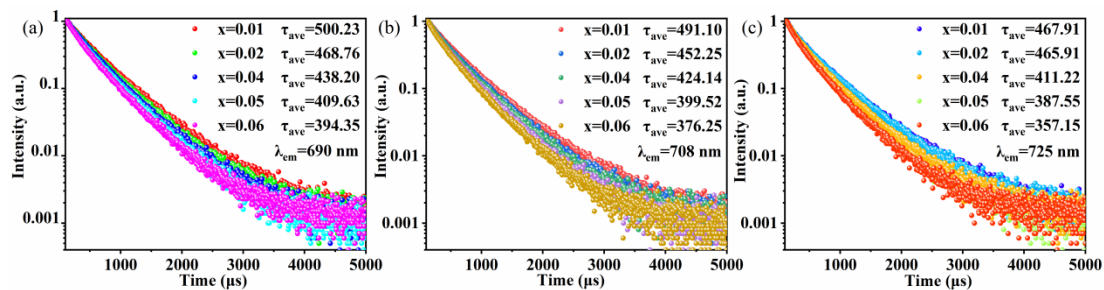


Figure S4. The decay curves of AG:xCr³⁺ under the excitation of 445 nm (a) the emission of 690 nm; (b) the emission of 708 nm; (c) the emission of 725 nm.

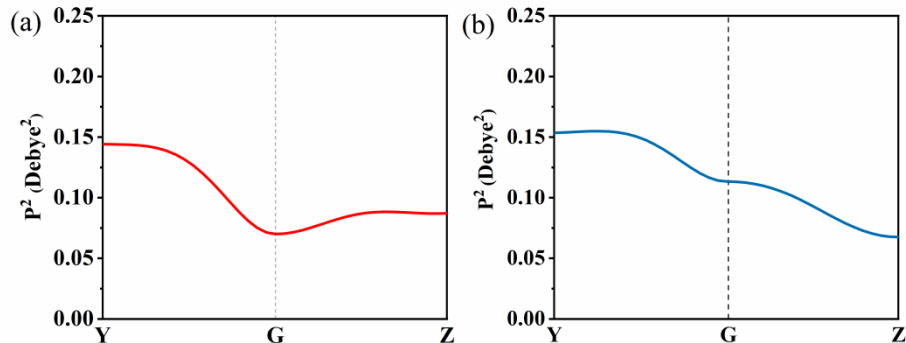


Figure S5. The transition dipole moments of (a) AG:0.05Cr³⁺; (b) A_{1.5}S_{0.5}G:0.05Cr³⁺

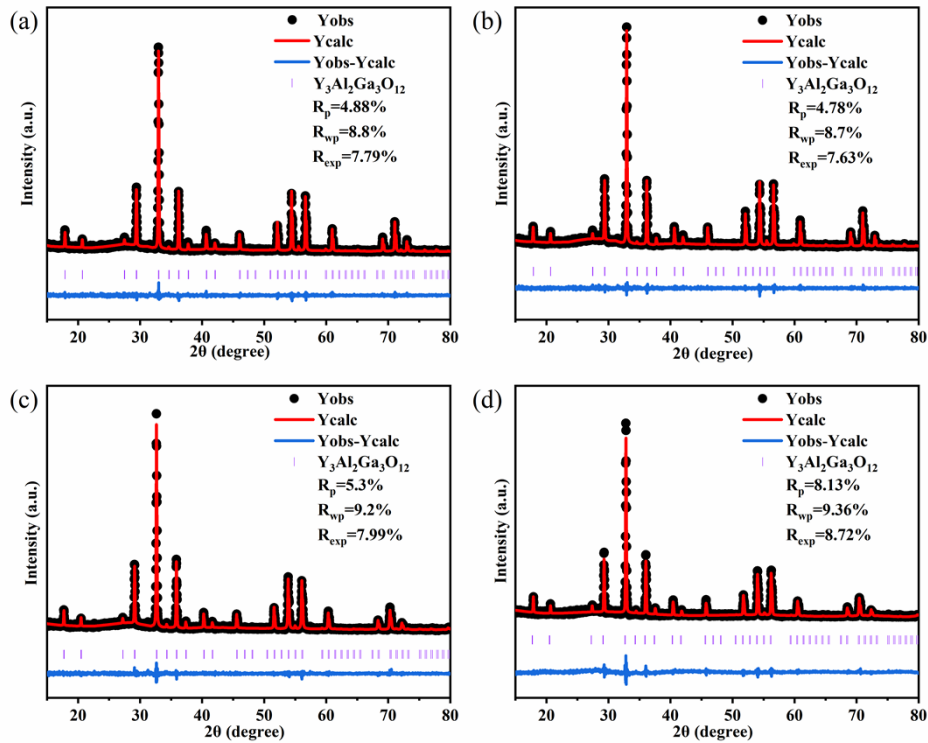


Figure S6. Rietveld refinement XRD patterns of $A_{2-y}S_yG:0.05\text{Cr}^{3+}$ at different temperatures (a) $y = 0$, $T = 298\text{ K}$; (b) $y = 0$, $T = 423\text{ K}$; (c) $y = 0.5$, $T = 298\text{ K}$; (d) $y = 0.5$, $T = 423\text{ K}$.

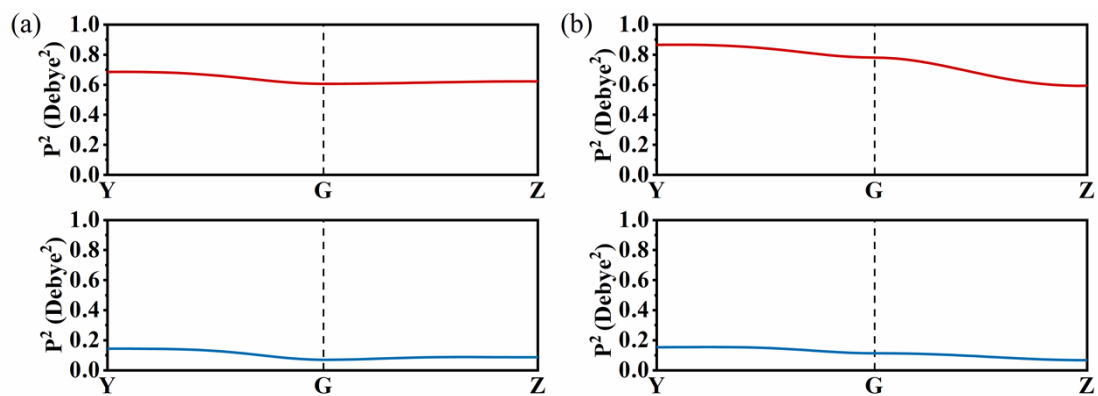


Figure S7. (a) The transition dipole moments of the normal octahedron(below) and the distorted octahedron(above) in $AG:0.05\text{Cr}^{3+}$; (b)The transition dipole moments of the normal octahedron(below) and the distorted octahedron(above) in $A_{1.5}S_{0.5}G:0.05\text{Cr}^{3+}$

Table S1. Crystal field parameters $A_{2-y}S_yG:0.05Cr^{3+}$

y	$^4A_2 \rightarrow ^4T_2$ (cm^{-1})	$^4A_2 \rightarrow ^4T_1$ (cm^{-1})	D_q (cm^{-1})	D_q/B
0	16420 (609 nm)	22272 (449 nm)	1527	2.65
0.3	16287 (614 nm)	22173 (451 nm)	1521	2.61
0.5	16207 (617 nm)	22124 (452 nm)	1500	2.55
0.7	15949 (627 nm)	220264 (454 nm)	1487	2.43
0.9	15823 (632 nm)	21930 (456 nm)	1467	2.37
1.2	15699 (637 nm)	21834 (458 nm)	1454	2.33
1.7	15625 (640 nm)	21739 (460 nm)	1448	2.32
2	15552 (643 nm)	21739 (460 nm)	1437	2.26

Table S2. The average lifetime calculation parameters of $A_{2-y}S_yG:0.05 Cr^{3+}$

y	A_1	τ_1	A_2	τ_2	τ_{ave}
0	1.36	144.70	0.55	465.16	325.68
0.3	1.31	149.79	0.64	355.76	260.59
0.5	1.71	152.26	0.35	318.54	202.53
0.7	1.97	126.50	0.48	245.11	164.51
0.9	2.34	122.17	0.31	229.76	143.54
1.2	2.73	107.73	0.27	191.85	120.40
1.7	3.08	101.02	0.18	189.97	109.60
2	3.35	96.39	0.12	205.86	104.34

Table S3. Rietveld crystallographic parameters of $A_{2-y}S_yG:0.05\text{Cr}^{3+}$ at different temperatures

y	Temperature (K)	Crystal system	Space group	$a=b=c$ (Å)	Volume (Å ³)	$\alpha=\beta=\gamma$ (°)
0	298	Cubic	Ia-3d	12.1480	1792.7277	90
0	423	Cubic	Ia-3d	12.1547	1796.9815	90
0.5	298	Cubic	Ia-3d	12.2644	1844.7557	90
0.5	423	Cubic	Ia-3d	12.2685	1846.6068	90

Table S4. Mechanical parameters of $A_{2-y}S_yG:0.05\text{Cr}^{3+}$ at different temperatures

parameters	$y=0,$ T=298 K	$y=0,$ T=423 K	$y=0.5,$ T=298 K	$y=0.5,$ T=423 K
Bulk modulus B_H (Gpa)	199.38	192.40	171.51	170.77
Young's Modulus E (GPa)	244.63	243.75	233.28	232.92
Shear Modulus G (GPa)	94.80	94.56	91.60	91.51
Poisson's Ratio ν	0.29	0.29	0.27	0.27
P-wave Modulus (Gpa)	320.78	318.49	293.65	292.78
Pugh's Ratio (B/G)	2.05	2.03	1.87	1.87
Vickers Hardness (GPa)	9.30	9.39	10.40	10.45
Volume (Å ³)	1792.73	1796.98	1844.76	1846.61
The number of atoms N	160	160	160	160
Debye temperature Θ_D (K)	624.5	623.7	615.3	615.0

Table S5. Thermal stability and Θ_D of several phosphors

Host	Active	Θ_D	$I_{423\text{ K}}/I_{298\text{ K}}(\%)$	Refs.
$\text{Lu}_3\text{Al}_5\text{O}_{12}$	Ce^{3+}	60	103	8
$\text{Sr}_2\text{LiAlO}_4$	Eu^{2+}	46	88	9
$\text{BaZrSi}_3\text{O}_9$	Eu^{2+}	49	77	10
$\text{Ba}_2\text{MgSi}_2\text{O}_7$	Eu^{2+}	38	~80	11
Sr_3SiO_5	Eu^{2+}	39	~75	12
ScF_3	Cr^{3+}	53	86	13
GaTaO_4	Cr^{3+}	56	60	14
$\text{LiInSi}_2\text{O}_6$	Cr^{3+}	55	77	15
$\text{Y}_3\text{In}_2\text{Ga}_3\text{O}_{12}$	Cr^{3+}	59	100	16
$\text{BaY}_2\text{Al}_2\text{Ga}_2\text{SiO}_{12}$	Cr^{3+}	62	108	This work
$\text{BaY}_2\text{Al}_{1.5}\text{Sc}_{0.5}\text{Ga}_2\text{Si}$	Cr^{3+}	61	104	This work

References

- 1 P. E. Blochl, *Phys. Rev. B: Condens. Matter Mater. Phys.*, 1994, **50(24)**, 17953-17979.
- 2 Perdew, *Phys. Rev. Lett.*, 1996, **77(18)**, 3865-3868;
- 3 J. D. Pack, H. J. Monkhorst, *Phys. Rev. B*, 1977, **16(4)**, 1748.
- 4 X. Q. Chen, H. Niu, D. Li, Y. Li, *Intermetallics*, 2011, **19(9)**, 1275-1281.
- 5 R. Gaillac, P. Pullumbi, F.-X. Coudert, *J. Phys.: Condens. Matter*, 2016, **28(27)**, 275201.
- 6 A. Marmier, Z. A. D. Lethbridge, R. I. Walton, C. W. Smith, S. C. Parker, K. E. Evans, *Comput. Phys. Commun.*, 2010, **181(12)**, 2102-2115.
- 7 V. Wang, N. Xu, J. C. Liu, G. Tang, W. T. Geng, *Comput. Phys. Commun.*, 2021, **267**, 108033.
- 8 T. W. Kang, K. W. Park, J. H. Ryu, S. G. Lim, Y. M. Yu, J. S. Kim, *J. Lumin.*, 2017, **191**, 35-39.
- 9 Z. Wang, J. Ha, Y. H. Kim, W. B. Im, J. McKittrick, S. P. Ong, *Joule*, 2018, **2(6)**, 914-926.
- 10 T. Komukai, Y. Takatsuka, H. Kato, M. Kakihana, *J. Lumin.*, 2015, **158**, 328-332.
- 11 X. Zhang, J. Zhang, R. Wang, M. Gong, *J. Am. Ceram. Soc.*, 2010, **93(5)**, 1368-1371.
- 12 J. Qiao, J. Zhao, Q. Liu, Z. Xia, *J. Rare Earths*, 2019, **37(6)**, 565-572.
- 13 Q. Lin, Q. Wang, M. Liao, M. Xiong, X. Feng, X. Zhang, H. Dong, D. Zhu, F. Wu, Z. Mu, *ACS Appl. Mater. Interfaces.*, 2021, **13(15)**, 18274-18282.
- 14 J. Zhong, Y. Zhuo, F. Du, H. Zhang, W. Zhao, S. You, J. Brgoch, *Adv. Opt. Mater.*, 2022, **10(2)**, 2101800.
- 15 X. Xu, Q. Shao, L. Yao, Y. Dong, J. Jiang, *Chem. Eng. J.*, 2020, **383**, 123108.
- 16 C. Li, J. Zhong, *Chem. Mater.*, 2022, **34(18)**, 8418-8426.